THE JOURNAL OF PHYSICAL CHEMISTRY B

Article

pubs.acs.org/JPCB

A Benchmark of Excitonic Couplings Derived from Atomic Transition Charges

Kurt A. Kistler,*[,†] Francis C. Spano, and Spiridoula Matsika[‡]

Department of Chemistry, Temple University, Philadelphia, Pennsylvania 19122, United States

ABSTRACT: In this report we benchmark Coulombic excitonic couplings between various pairs of chromophores calculated using transition charges localized on the atoms of each monomer chromophore, as derived from a Mulliken population analysis of the monomeric transition densities. The systems studied are dimers of 1-methylthymine, 1-methylcytosine, 2-amino-9-methylpurine, *all-trans*-1,3,5-hexatriene, *all-trans*-1,3,5,7-octatetraene, *trans*-stilbene, naphthalene, perylenediimide, and dithia-anthracenophane. Transition densities are taken from different single-reference electronic structure excited state methods: time-dependent density functional theory (TDDFT), configuration-interaction singles (CIS), and semiempirical methods based on intermediate neglect of differential overlap. Comparisons of these results with full ab initio calculations of the electronic couplings using a supersystem are made, as are comparisons with experimental data. Results show that the transition charges do a good job of reproducing the supersystem couplings for dimers with moderate to long-range interchromophore separation. It is also found that CIS supermolecular couplings tend to overestimate the couplings, and often the transition charges approach may be better, due to fortuitous cancellation of errors.

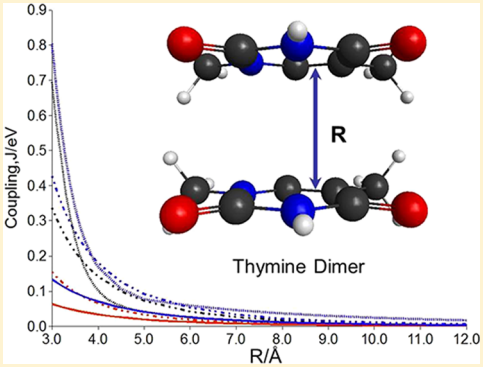

1. INTRODUCTION

The ability to accurately model the electronic coupling between interacting chromophores or aggregates of interacting chromophores is of great value for designing nanoscale photonic devices, such as optical switches,[1,2] and understanding biological processes such as light harvesting in photosynthesis[3,4] and DNA photostability.[5] The main mechanism by which energy is transported between chromophores subsequent to photoexcitation involves excitons, in which the molecular excitations are generally delocalized over several chromophores.

Although high-level ab initio calculations might be a preferred way to theoretically study the excited states of groups of chromophores, such a venture quickly becomes too computationally expensive for all but a limited number of very small chromophores, whereas the typical aggregate in optical devices can be an extremely large ensemble, made up of large polyaromatic systems. The Frenkel exciton model[6] simplifies the analysis by assuming that an aggregate's spectral properties can be determined from the electronic properties of the individual chromophores and the interactions between individual electronically excited states. The latter is often referred to as excitonic coupling.

The simplest model to calculate the excitonic coupling is to restrict the interaction between the monomers to the Coulombic interaction, and represent it with the dipole transition moments of the two molecules. This is now commonly known as the point dipole approximation (PDA). Although PDA is simple, convenient, and computationally cheap, it breaks down when the distance between chromophores is less than the spatial extent of the transition dipole moment. The Coulomb interaction between the chromophores can be extended beyond the dipole−dipole approximation to incorporate multipole couplings, which have been found to contribute significantly to the Coulombic coupling for short intermolecular distances.[7,8] An even better approach is to evaluate the complete Coulomb interaction using the transition densities describing the excitation from the ground to the excited state in the monomer. This has been done by decomposing the transition density in a three-dimensional grid and then calculating the Coulomb interaction via pairwise charge−charge interactions. This approach is known as the density cube method.[9] Alternatively, one can calculate the Coulomb coupling directly using the integrals obtained from ab initio codes.[10−13]

A more cost-effective and accessible method of modeling the Coulomb coupling is to decompose the transition density into point charges localized on the atoms.[8,13−21] Different approaches exist to calculate atomic charges on the basis of the density or transition density. One method, similar to the Mulliken population analysis (MPA), uses the density to obtain populations centered on the atomic nuclei and converts these populations into charges, called transition charges (tq's). The density can be obtained by a variety of methods, either semiempirical or ab initio. Atomic charges can be obtained by other methods besides population analysis. A quite accurate method, which has been used extensively for the ground state to determine charges, involves fitting the electrostatic potential around the molecule. This method has now been applied to

Received: October 25, 2012
Revised: January 11, 2013
Published: February 7, 2013

   dx.doi.org/10.1021/jp310603z | *J. Phys. Chem. B* 2013, 117, 2032−2044

tq's, using electrostatic potentials of the different states and the transition.[19]

The interaction between chromophores is not limited to the Coulomb interaction. The quantum mechanical properties that completely describe the interaction of two molecular systems include, in addition to Coulomb interactions, exchange, orbital overlap, and state mixing when a chromophore has multiple excited states in close energetic proximity, and much work has gone into the dissection of a full electronic structure into these components.[10,22−26] These are very useful studies in giving insight into the contribution of the different components of the coupling, and in obtaining more accurate couplings.

Regardless of the approximate nature of tq's, they can be very useful in studies of aggregates, where other methods are too expensive. So, a more careful assessment of the accuracy of tq-based methods is needed. In this work we investigate the transition charges generated by a variety of electronic structure methods and basis sets and determine how well they can reproduce the Coulomb coupling. Several molecules have been investigated that belong to two general categories, either aromatic molecules with heteroatoms, such as the nucleobases, or conjugated hydrocarbons. It will be shown that the performance of the various methods depends on the type of molecule and type of excited states involved. The couplings are compared to couplings generated using the supersystem of the two interacting chromophores.

In what follows, we present the theory and mathematical description of calculating tq's using MPA of the transition density in section 2. In the following section we will present the computational details of the methods used for this study. Results of excitonic couplings calculated using MPA-derived tq's from the transition densities of a variety of single-excitation methods will be discussed in section 4 and compared to dimer supermolecular couplings. We will also compare these theoretical methods with experimental data of two different molecular systems. Finally, we will summarize this report in section 5. Because of the high density of acronyms in this work, a list of all acronyms is included.

2. THEORY

In the Frenkel exciton model,[6] an aggregate of interacting chromophores has an excited state wave function, Ξ, written in terms of a linear combination of excited state wave functions, Ψ^{e}_{m}, where excitation is localized to an individual chromophore m, such that

$$\Xi = \sum_{m}^{N_{\text{monomers}}} C_m \Psi^{e}_{m} \tag{1}$$

where m is the index over monomer chromophores and C_m is the contribution to the exciton state. Ψ^{e}_{m} is a product of the monomer chromophore wave functions, ψ_m, given as

$$\Psi^{e}_{m} = \psi^{e}_{m} \prod_{k\neq m}^{N_{\text{monomers}}} \psi^{0}_{k} \tag{2}$$

where ψ^{e}_{m} and ψ^{0}_{m} are the electronic excited and ground state wave functions of individual chromophore m, respectively. The requirement that the wave function is antisymmetric with respect to interchanging electrons between two different chromophores has been ignored here. This is equivalent to ignoring the exchange terms and focusing only on the Coulomb interaction. The Hamiltonian of the aggregate system, H, is given as the sum of individual chromophore Hamiltonians, H_m, as an unperturbed part, along with a perturbation, as

$$H = \sum_{m}^{N_{\text{monomers}}} H_m + \sum_{m}\sum_{l>m} V_{ml} \tag{3}$$

where V_{ml} is the Coulomb operator, given in atomic units as

$$V_{ml} = \sum_{i}^{n_m}\sum_{j}^{n_l} \frac{1}{|\mathbf{r}_i - \mathbf{r}_j|} \tag{4}$$

Here i and j are indices of the electrons of chromophore m and l, respectively, and $\mathbf{r}_i$ and $\mathbf{r}_j$ are their positions. n_m and n_l are the number of electrons for chromophore m and l, respectively. In this framework, the Coulombic excitonic coupling between chromophore m and l, J_{ml}, is the off-diagonal element of the exciton Hamiltonian matrix, given as

$$J_{ml} = \langle \Psi^{e}_{m} | H | \Psi^{e}_{l} \rangle = \langle \psi^{e}_{m} \psi^{0}_{l} | V_{ml} | \psi^{0}_{m} \psi^{e}_{l} \rangle \tag{5}$$

which, in the formalism of Longuet−Higgins,[17,18,27] can be written in terms of the transition densities, ρ^{t} as

$$J_{ml} = \int\int \frac{\rho^{m,t}(\mathbf{r})\, \rho^{l,t}(\mathbf{r}')}{|\mathbf{r} - \mathbf{r}'|}\, d\mathbf{r}\, d\mathbf{r}' \tag{6}$$

The coupling J_{ml} can be thought of as the electrostatic interaction between the transition densities of chromophores m and l, $\rho^{m,t}$ and $\rho^{l,t}$. In this treatment we also assume that only one excited state of each monomer participates in the coupling.

Though such a description would have far more spatial resolution than the much cruder PDA, where the interaction is simply between two point transition dipole vectors, it can be a rather expensive and computationally difficult model to create. The approach is simplified if these transition densities can be decomposed to atomic tq's by building the transition density from an ab initio calculation. Now J_{ml} can be written in terms of these tq's, which are given in the equation as q^{t}, such that

$$J_{ml} = \sum_{i}^{N_m}\sum_{j}^{N_l} \frac{q^{t}_{i} q^{t}_{j}}{|\mathbf{R}^{m}_{i} - \mathbf{R}^{l}_{j}|} \tag{7}$$

Here $\mathbf{R}^{m}_{i}$ is the position of atom i of chromophore m, and N_m is the number of atoms in chromophore m. If the density is obtained from a semiempirical approach, such as ZINDO (Zerner's intermediate neglect of differential overlap), where the basis set is a minimal Slater-type atomic orbital (STO) basis of ortho-normal functions, the transition charge associated with atom P can be calculated from a configuration interaction singles (CIS) expansion as[17]

$$q^{t}_{P} = \sqrt{2} \sum_{b}^{N_{\text{AO},P}} \sum_{j}^{\text{unocc}} \sum_{i}^{\text{occ}} A_{ij} c^{Pb}_{i} c^{Pb}_{j} \tag{8}$$

where i is the index of occupied molecular orbitals (MOs) being excited from, j is the index of virtual unoccupied MOs being excited to, b is the index of the atomic orbital (AO) basis function, χ_{Pb}, for each MO centered on atom P, $N_{\text{AO},P}$ is the number of AO basis functions centered on atom P, c^{Pb}_{i} is the AO coefficient b of MO ϕ_i centered on atom P, such that $\phi_i = \sum_{P,b} c^{Pb}_{i} \chi_{Pb}$, and A_{ij} is the CI coefficient from the CIS calculation corresponding to excitation from ϕ_i to ϕ_j. The form of this equation assumes that the basis set is ortho-normal, such as the STO-AOs in the ZINDO method, and electron transitions do not occur between different atoms on the chromophore, rather

dx.doi.org/10.1021/jp310603z | J. Phys. Chem. B 2013, 117, 2032−2044

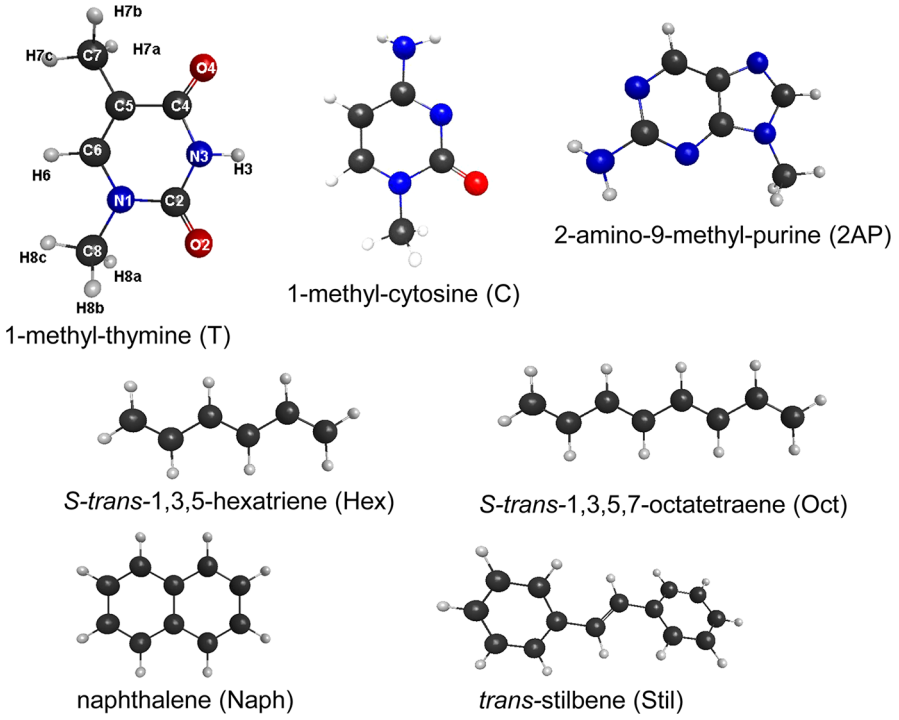

Figure 1. Structures of molecules presented in this study, along with their names and abbreviations used.

they are completely localized on a single atom *P*. Two criteria for the tq's must be met: for a particular chromophore their sum must be zero, and when taken with their atomic positions, the resulting vector should equal the transition dipole, μ, mathematically given as

$$\sum_{P=1}^{N_m} q_P^t = 0 \qquad \boldsymbol{\mu} = \sum_{P=1}^{N_m} q_P^t \mathbf{R}_P \tag{9}$$

The assumptions for eq 8 make the calculation of tq's quite simple and convenient, but they are also very limiting. When one moves from semiempirical methods to other single-reference ab initio methods, this equation has to be adjusted because the basis sets used are not necessarily orthogonal anymore. The form of this transition density MPA in that case is given as

$$q_P^t = \sqrt{2} \sum_{b}^{N_{AO,P}} \sum_{c}^{N_{AO}} \sum_{j}^{unocc} \sum_{i}^{occ} A_{ij} c_i^{Pb} c_j^c S_{bc} \tag{10}$$

where N_{AO} is the number of all AOs, and all other notations have been defined earlier.

One can see in eq 10 that CI transition determinants are now included that describe both intra- and interatom excitations, and the inclusion of overlap S at the AO level allows for the use of more robust AO basis sets than the minimal basis set used at the ZINDO level. Requirements for using eq 10 on the results of a CIS calculation are obtaining the **S** matrix, the MO matrix of AO coefficients, and the printing of CI coefficients to a low threshold value, that is, obtaining as many CI coefficients for a particular excited state as possible. In addition, as long as these quantities can be obtained, eq 10 holds for CIS, TDDFT, and ZINDO excited state methods, allowing comparisons of results between them. In this study we used Gaussian 03[28] to extract the information needed to build the charges. Although not available at the time we did this study, the most recent version of Gaussian (Gaussian 09[29]) includes a variation of this approach.

3. COMPUTATIONAL METHODS

The excited state electronic structure methods and basis sets used in this study will be described here. The chromophores chosen for this study are shown in Figure 1, along with their names and abbreviations used in this report. The atomic numbering of 1-methylthymine (T) is shown and follows the usual biochemistry numbering system for nucleobases, as do 1-methylcytosine (C) and 2-amino-9-methylpurine (2AP). For these three, methyls have replaced the ribose attachment they would have in actual DNA. The other systems are the all-trans conformers (*S-trans*) of 1,3,5-hexatriene (Hex) and 1,3,5,7-octatetraene (Oct), *trans*-stilbene (Stil), and naphthalene (Naph).

All molecules were optimized at the Møller–Plesset second-order perturbation theory level (MP2) using Dunning's cc-pVDZ basis set.[30] Face-to-face dimers of all the chromophores were created at various interchromophore distances. With T, because our main interest was on coupling in a B-DNA double helix, an additional set of geometries was investigated, as defined in Figure 2. Initially, the base-pair adenine–thymine with correct hydrogen bonding was optimized, with the base-pair approximately parallel to the *x,y*-plane. A duplicate of T was created parallel to it at a distance of *R* in the *z*-direction, face-to-face, and then this second base was rotated about the *z*-axis defined as going through the center of mass of the base pair by an angle θ. The other base of the base-pair was then removed. With R = 3.4 Å and θ = 35.9°, this dimer orientation closely approximates a stacked adjacent base dimer in one strand of the B-DNA double helix, a dimer orientation of high interest in the field of DNA photophysics. At R = 6.8 Å and θ = 71.8°, the dimer closely approximates the orientation of two bases in a B-DNA strand separated by one base pair. We will refer to this type of rotation of one base chromophore with respect to the other as B-DNA rotation.

dx.doi.org/10.1021/jp310603z | J. Phys. Chem. B 2013, 117, 2032–2044

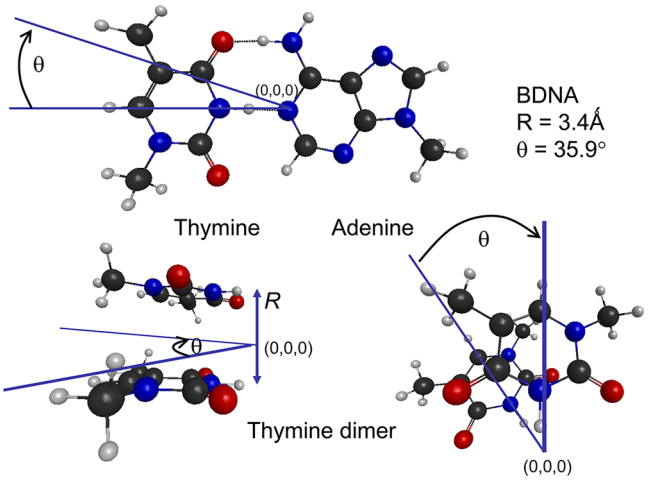

Figure 2. Graphical illustration of a B-DNA rotation, as described in section 3, for a T−T dimer, with the origin (0, 0, 0) defined as the center-of-mass of a thymine−adenine base-pair primarily in the *x,y*-plane. θ is the angle of rotation of the top T, also parallel to the *x,y*-plane, around the $z = 0$ axis, and R is the separation between the two T's and has the vector R parallel to the *z*-axis.

Various single reference methods were used to calculate the excited states of the molecules. Methods used were CIS, TDDFT using the B3LYP or PBE1PBE hybrid functionals, and ZINDO. ZINDO only uses one minimal ortho-normal STO basis set, but with CIS and TDDFT virtually all AO basis sets are available, and several were used for T, such as 3-21G, cc-pVDZ, cc-pVTZ, and aug-cc-pVDZ, to compare the effect of basis set size and influence of including diffuse functions on the coupling. CI coefficients $A_{ij} \geq 10^{-5}$ for the excited state of interest were used in calculating transition charges. Also, for each method and basis set, the corresponding matrices of the AO coefficients for the MOs and the overlap **S** were parsed and used. Equations 8 (for ZINDO) and 10 (for CIS and TDDFT) were used to obtain the charges, using information obtained from excited state calculations. Once each atom in the chromophore is assigned transition charges, it is a simple matter to construct dimer geometries numerically and calculate J_{ml} using eq 7. To compare the calculated couplings with ab initio results on the supermolecule, CIS and CIS with second-order perturbation theory corrections (CIS(2))[31] calculations on representative dimer geometries were carried out using the cc-pVDZ basis set. TDDFT dimer calculations were, in general, not carried out in this report due to the method's overstabilization of charge transfer states (CT), an erroneous artifact of the method. These CT states cross with the exciton states at shorter distances and mix with them, making identification of the exciton states difficult.[32] This is not a problem with the other methods listed above.

Most of the geometries in this study are symmetric, so it is easy to obtain the coupling from the energy gap between the supermolecule states. In the cases where the geometries are not symmetric the energy gap cannot be used directly, and there are several procedures to obtain the coupling.[33−35] Here, we use an Edmiston−Ruedenberg (ER) diabatization procedure, as implemented in QChem for CIS wave functions.[35,36] Very similar couplings were obtained with the fragment excitation difference approach[33] in selected cases that we chose to compare.

Excited state calculations to obtain tq's were carried out using the Gaussian03 quantum package,[28] geometry optimizations were done using GAMESS,[37] and molecular visualizations and manipulations were done using MOLDEN[38] and MacMolPlt.[39] CIS(2) is part of the Priroda suite of quantum programs by Laikov.[40]

4. RESULTS AND DISCUSSION

Unless otherwise specified, all molecules described in this section were in their closed-shell ground state geometry, optimized at the MP2/cc-pVDZ level, with their structures shown in Figure 1.

4.1. Monomer Properties. All ground and excited electronic states discussed here are singlet states, denoted as S_I, where I denotes the Ith excited state, starting with S_0, the ground state. Table 1 lists the calculated excited state electronic properties for the relevant state for all chromophores reported in this work. Because the behavior of the couplings depends on the character of the chromophore and its excited states, we briefly describe the systems we have included in this work. In general, we divide them in two groups. The first group consists of the nucleobases, with several heteroatoms in their rings, whereas the second group consists of conjugated hydrocarbons. Naphthalene is included in the study because its dimers have been studied extensively in the literature, and the exciton coupling has been benchmarked with various methods. This collection of systems gives enough variety in our benchmarking studies, and it also includes important systems, for which many scientists would be interested to know the couplings.

4.1.1. Nucleobases. The three nucleobases presented here have their lowest excited states as either $\pi\pi^*$ excitations or $n\pi^*$ ones. The $n\pi^*$ states have very small oscillator strengths, and they do not contribute significantly to the coupling between the bases, so we only consider the coupling from the $\pi\pi^*$ states here. The first $\pi\pi^*$ state is S_2 for T and S_1 for C and 2AP. The energies calculated at the CIS and CIS(2) level are overestimated compared to the experimental values, whereas TDDFT gives the best match for all three molecules. ZINDO underestimates the excitation energies, and in two cases does not even predict the correct ordering of the states.

What is more important for our studies, however, is the transition dipole moment for that transition. The calculated magnitude from electronic structure methods, denoted esTDP, is shown in Table 1 and compared to the experimental value. For this property there is much more variation in the performance of the different methods. CIS(2) gives the best value for T, ZINDO for C, and TDDFT for 2AP; thus one cannot draw any conclusions about the applicability of any of these methods for the transition dipole moments.

4.1.2. Conjugated Hydrocarbons. In these conjugated systems there are no heteroatoms, so there are no $n\pi^*$ states. There are, however, still dark states present, which are doubly excited states. A doubly excited state is experimentally the first excited state for both Hex and Oct. All the methods that we have used in this work, however, are single reference methods, and they cannot describe this type of excited state, so in our calculations the first excited state is the $\pi\pi^*$ state. The energy of the first excited $\pi\pi^*$ state in all cases for these hydrocarbons is predicted more accurately using the TDDFT approach when compared to experiment. The esTDPs calculated are in much larger disagreement with experiment compared to the nucleobases. The reason, however, may be in experimental fault rather than theoretical. For Hex the bright $\pi\pi^*$ S_2 state was experimentally measured in hexane by Gavin and co-workers,[41] where they reported an oscillator strength estimated at 0.74, but the

dx.doi.org/10.1021/jp310603z | J. Phys. Chem. B 2013, 117, 2032−2044

Table 1. Monomer Electronic Properties[a] for the Molecules in This Work

	E $\pi\pi^*$	state	esTDP	tqTDP	f
T					
CIS/cc-pVDZ	6.252	S_1	4.595	3.623	0.501
CIS(2)/cc-pVDZ	5.644	S_2	3.819		0.334
TDDFT/cc-pVDZ	4.957	S_2	3.056	2.795	0.176
ZINDO	4.417	S_3	4.837	4.439	0.392
expt[18,57]	4.8	S_2	3.68		0.24
C					
CIS/cc-pVDZ	5.936	S_1	3.081	2.307	0.214
CIS(2)/cc-pVDZ	5.024	S_1	2.394		0.110
TDDFT/cc-pVDZ	4.627	S_1	1.921	1.690	0.065
ZINDO	4.089	S_2	3.256	2.912	0.116
expt[18,58]	4.65	S_1	3.45		0.21
2AP					
CIS/cc-pVDZ	5.608	S_1	3.973	3.281	0.336
CIS(2)/cc-pVDZ	5.012	S_1	3.229		0.198
TDDFT/cc-pVDZ	4.392	S_1	2.749	2.609	0.126
ZINDO	3.976	S_1	4.118	3.771	0.256
expt[59]	4.068	S_1	2.546		0.10
Hex					
CIS/cc-pVDZ	5.509	S_1	9.022	6.799	1.700
CIS(2)/cc-pVDZ	5.723	S_1	8.427		1.541
TDDFT/cc-pVDZ	4.797	S_1	7.620	6.415	1.056
ZINDO	4.351	S_1	8.878	8.452	1.301
expt (hexane, 0−0)[41]	4.92	S_2	6.3		0.74
expt (gas, max is 1−0 transition)[60]	5.13	S_2			
Oct					
CIS/cc-pVDZ	4.831	S_1	11.048	8.555	2.236
CIS(2)/cc-pVDZ	5.001	S_1	10.685		2.114
TDDFT/cc-pVDZ	4.095	S_1	9.723	8.414	1.468
ZINDO	3.785	S_1	10.849	10.469	1.689
expt (hexane, 0−0)[42]	4.40	S_2	4.490		0.336
expt (gas phase, 0−0)[61]	4.42	S_2			
Stil					
CIS/cc-pVDZ	4.889	S_1	7.438	5.753	1.026
CIS(2)/cc-pVDZ	5.089	S_1	8.004		1.236
TDDFT/cc-pVDZ	4.191	S_1	7.562	6.398	0.909
ZINDO	3.996	S_1	8.166	7.972	1.011
expt (3-methylpentane)[62]	4.22		6.8		0.74
Naph					
CIS/cc-pVDZ	5.108	S_1	2.073	1.858	0.083
CIS(2)/cc-pVDZ	5.38	S_2	2.382		0.116
TDDFT/cc-pVDZ	4.462	S_1	1.922	1.982	0.063
ZINDO	4.151	S_2	3.043	2.652	0.146
expt[63,64]	4.43	S_2	3.27		0.18

[a]Excitation energies E (eV), magnitude of the transition dipole moment, esTDP (D), and oscillator strengths f. The magnitude of the transition dipole moment from tq's derived from these methods are also shown (tqTDP, D).

authors state it may be somewhat higher. For Oct, as well, the oscillator strength from experiment, given as 0.34,[42] is almost certainly too low, as it is expected to be higher than that of Hex, but no reports of correcting this have been found. Given this, the estimated TDP, 4.49 D, is also almost certainly too low. Given the possible underestimation of experimental values, the theoretical values may be more accurate than they appear here.

Overall, the performance of each method to describe the monomer properties varies widely with the system. This performance will have an effect on the calculated couplings as well. The uncertainty that exists in the experimental TDP makes benchmarking these properties difficult.

4.2. Transition Charges and Their Ability To Reproduce Transition Dipole Moments. We first examine the behavior of the transition charges calculated and how they can reproduce the transition dipole moments. Figure 3 shows

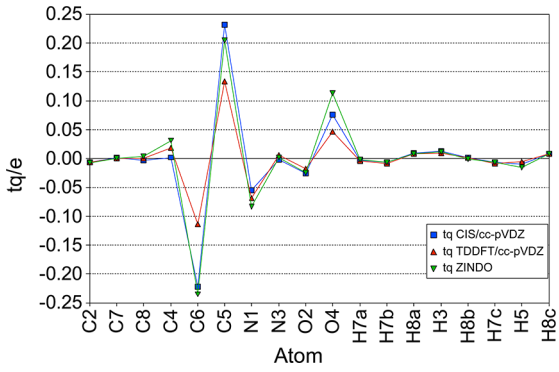

Figure 3. Transition charges for T, calculated at the CIS and TDDFT levels, using the cc-pVDZ basis set, and at the ZINDO level, shown for each atom, according to the numbering defined in Figure 1.

the tq's for T calculated using CIS, TDDFT, and ZINDO. The TDP for each of these three methods can be calculated using eq 9, denoted as tqTDP, and compared to that calculated directly from the wave function of the corresponding excited state monomer. These values are given in Table 1. Unlike a static state dipole moment, which has a single orientation and direction based on distortion of the density of the state, the TDP vector has a single orientation but can be of arbitrary direction, because the wave functions of the two states involved in the transition have arbitrary signs. Thus the TDP vector is often graphically shown as a double-headed arrow. Consequently, the sign of the derived tq's is also arbitrary, but the relative sign between the charges on the atoms of the same molecule is unique. Whenever we compare tq's derived from different methods, we make sure they have consistent signs. Furthermore, inverting the signs of all tq's of a molecule does not change the exciton coupling. For T, Figure 3 shows a relative pattern typical of the tq's calculated by these three methods. When comparing the ab initio TDPs (esTDPs) for the different electronic structure methods, ZINDO, in general, predicts a TDP with the largest magnitude, TDDFT predicts the smallest, and CIS is somewhere between. This trend is correspondingly seen in the tq's, where tq's that are positive (negative) will generally be most positive when calculated with ZINDO, and generally least positive (negative) when calculated with TDDFT, with tq's calculated with CIS in general being somewhere between the other two. In some cases the charges may differ by a factor as large as 2, as is seen for C5 and C6.

In principle, the transition charges should reproduce the ab initio transition dipole moments obtained from the same method. In reality, the magnitude of the tqTDPs tends to be lower than that of the esTDP. The deviation is the largest for the CIS tq's where on average (based on the systems studied here) the magnitude is 20% lower than the corresponding magnitude of esTDP obtained using CIS. The deviation is smaller for TDDFT tq's, on average 12% lower, and even smaller for ZINDO tq's, where it is only 6% smaller than the magnitude obtained from the wave function. Although this deviation reflects an error of the Mulliken analysis, it turns out that it

dx.doi.org/10.1021/jp310603z | J. Phys. Chem. B 2013, 117, 2032−2044

fortuitously serves to cancel the overestimation of the magnitude of the transition dipole moments obtained from the ab initio methods used here. It is not clear why the deviation is so different between the different methods.

Though a tqTDP from MPA has a smaller magnitude compared to the esTDP, the orientation predicted by the charges is very similar to the ab initio one. It should be noted that, in a similar fashion, MPA on the ground state density gives partial atomic charges that most often qualitatively predict an accurate ground state dipole, in terms of orientation, but with an inaccurate prediction of its magnitude.[43]

4.3. Couplings as a Function of Interchromophore Distance. We now look at the couplings calculated using the derived transition charges and how they compare to those obtained by other methods. We first examine the functional behavior of the couplings as a function of distance between the two chromophores. The exciton coupling was calculated using the tq's of the first excited $\pi\pi^*$ state of each monomer or by using the transition dipole moment of that state. These values were compared to the coupling obtained from the supersystem as half the energetic splitting of the two $\pi\pi^*$ states. The supersystem calculations used CIS and CIS(2) whereas monomer tq's were obtained from CIS, CIS(2), and TDDFT. PDA results were obtained using the esTDPs from CIS, CIS(2), and TDDFT. Because CIS(2) is the highest level of theory in this report, and because experimental couplings are not available for these systems, the results of CIS(2) supermolecular calculations will act as a reference. Figures 4, 5, and 6 show the exciton coupling, J, calculated using the various approximations for T, 2AP, and Hex, respectively.

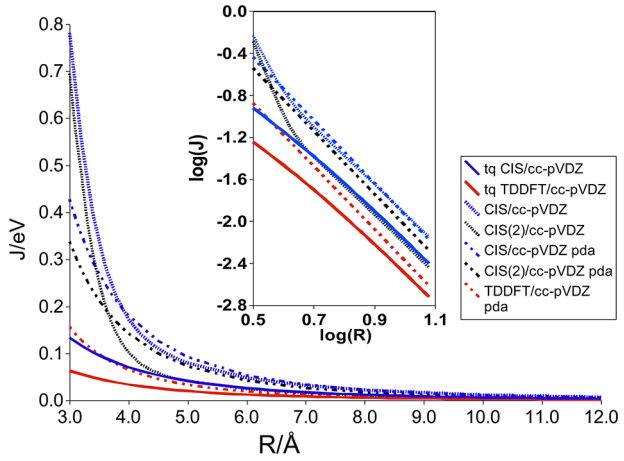

Figure 4. Exciton coupling J (eV) shown for face-to-face T dimer with respect to separation distance R (Å). Solid lines show the coupling calculated using the tq's, course-dashed lines show the coupling calculated using the PDA, and fine-dashed lines correspond to the coupling obtained from the supersystem calculations. The inset shows the log(J) vs log(R) plot.

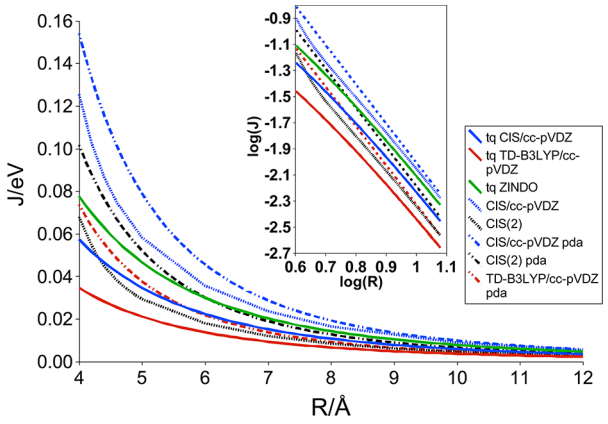

Figure 5. Exciton coupling J (eV) shown for face-to-face 2AP dimer with respect to separation distance R, from 4 to 12 Å. Solid lines show the coupling calculated using the tq's, course-dashed lines show the coupling calculated using the PDA, and fine-dashed lines correspond to the coupling obtained from the supersystem calculations. The inset shows the log(J) vs log(R) plot.

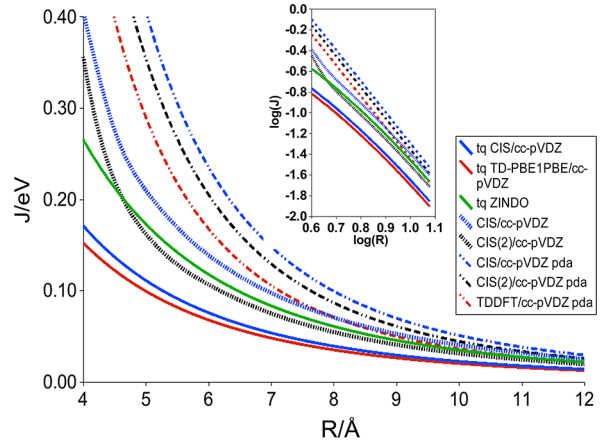

Figure 6. Exciton coupling J (eV) shown for face-to-face Hex dimer with respect to separation distance R. Solid lines show the coupling calculated using the tq's, course-dashed lines show the coupling calculated using the PDA, and fine-dashed lines correspond to the coupling obtained from the supersystem calculations. The inset shows the log(J) vs log(R) plot.

In T the coupling is shown starting from R = 3 Å so that the deviation from the Coulombic interactions is obvious. As is seen in Figure 4, there is variation in the coupling depending on the method used. At R > 4.5 Å tq's from CIS predict J values virtually matched with the supermolecular CIS(2) J, with J from TDDFT tq's consistently lower than J from CIS tq's, reflecting the lower esTDP of TDDFT. Couplings using PDA and esTDPs from CIS, CIS(2), and TDDFT are also shown and reflect the relative magnitudes for each of these esTDPs, with CIS PDA displaying the highest of the three. PDA couplings using the esTDP of CIS(2) is lower than that of CIS, whereas PDA using the esTDP of TDDFT gives J very close to J from CIS tq's.

The inset shows the plots of log(J) vs log(R). These plots are linear and the slope indicates the polynomial dependence of the coupling on R. For PDA methods the slope is exactly −3, indicating the R^{-3} dependence. For the couplings generated with tq's, the line has a somewhat smaller slope, between −2.57 and −2.58 in T. The slight downward curve for the log(J) plots with increasing R indicates an R^{-3} dependence would be approached at very large R. Interestingly, even though there is variation in the actual couplings depending on the source of the tq's, the slopes of the curves are almost identical for the different methods. The coupling calculated by the splitting of the energies in the supersystem shows a different behavior, because it changes slope dramatically around R = 4.5 Å, when effects beyond the Coulomb coupling become important. The slope for distances less than 4 Å becomes closer to −5 or −6.

dx.doi.org/10.1021/jp310603z | J. Phys. Chem. B 2013, 117, 2032−2044

Figure 5 shows the calculated exciton couplings for a face-to-face 2AP dimer with varying separation distance R. The behavior is similar to T although the CIS tq's do not do as well for 2AP as they did for T, whereas the TDDFT tq's do better. In 2AP the logarithmic plots show that the exponential dependence is between −2.71 and −2.74 for the couplings calculated using tq's. Again, the slope is almost the same regardless of the method used to generate the tq's, and overall the slope is somewhat smaller than the one predicted from the dipole dipole interaction, (i.e., −3).

Figure 6 shows the face-to-face coupling for the Hex dimer with respect to separation distances R from 4 to 12 Å. Because the tqTDP using ZINDO is almost equal to the esTDP from CIS(2), one could expect the couplings from these two methods to be also well-matched, and this is the case for all but very close distances. So, in this case the ZINDO tq's agree best with the ab initio coupling. For Hex the logarithmic plots show an exponential dependence of the coupling with respect to the distance with exponent −2.40.

Overall, it seems that the transition charges can reproduce the coupling of the supersystem, and its R dependence, quite well, but the actual accuracy depends on the system. The charges and couplings derived from different ab initio or semiempirical methods depend on the method used, and no method is universally better than the others. Which one will do better is heavily system dependent. More discussion on the performance of the charges overall will be given in section 4.5. The exact functional dependence also depends on the chromophore. The larger the actual coupling (as in Hex), the larger the deviation of the exponent from the PDA value of −3 becomes for the intermediate distances discussed here. For very large R PDA is expected to work well, whereas for smaller R both PDA and tq's will fail.

4.4. Basis Set Effect. To investigate how the basis set can affect the tq's, we examined several basis sets in the T−T face-to-face coupling. Figure 7 shows the coupling using CIS tq's with the Gaussian basis sets 3-21G, cc-pVDZ, cc-pVTZ, and aug-cc-pVDZ, which includes diffuse functions for all atoms. Also, included in the plot is ZINDO/STO-3G. The largest difference is with ZINDO/STO-3G, but it is most likely that this is due to the semiempirical nature of the INDO Hamiltonian rather than the minimal nature of STO-3G. The results with the Gaussian basis sets show only modest difference between each other, even at very short range, but a general trend of the smallest basis, 3-21G, giving the highest |tq|, and thus higher couplings, with the effect of increasing basis set size diminishing |tq| and thus the corresponding couplings. It is perhaps a welcome observation that this trend is quite minimal, because it implies that the study of coupling between very large chromophore systems using tq's would not necessarily require very expensive basis sets to derive the tq's. The fact that inclusion of diffuse functions has a minimal effect on calculated exciton coupling has been seen before as well.[31] Indeed, it is the method itself that has the largest influence on calculated dimer couplings. This insensitivity of calculated coupling from tq's to basis set changes was also observed with the other chromophore dimer systems presented in this study, for both CIS and TDDFT tq's, even though the results are not shown here.

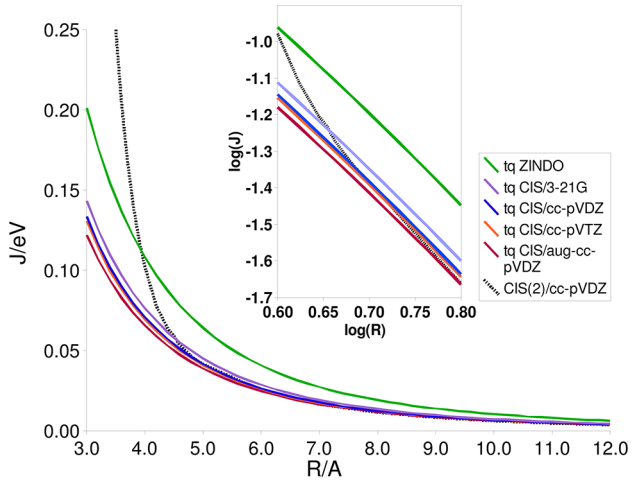

Figure 7. Exciton coupling (eV) shown for face-to-face T dimer with respect to separation distance R (Å), as calculated using ZINDO, CIS/3-21G, CIS/cc-pVDZ, CIS/cc-pVTZ, and CIS/aug-cc-pVDZ. Also shown is the CIS(2) coupling for comparison. The inset shows the log(J) vs log(R) plot.

The basis set effect on the coupling has been examined before for various methods using the supermolecular approach. It was found, in agreement with our results, that there is minimal dependence on the basis set.[44]

4.5. Comparisons between the Different Methods. A more systematic comparison between the different methods used here to obtain the couplings is discussed in this section. Table 2 shows the coupling at three different distances as obtained by the different approaches used here for all the molecules in our list. Table 3 shows the percent deviation (% dev) of the coupling at the same three distances compared to the CIS(2) supersystem coupling.

Before checking the performance of the model methods to get the coupling, we will compare the results of the supersystem calculations using the two different ab initio methods, CIS and CIS(2). The difference between these two methods is the incorporation of dynamical correlation with CIS(2), which is absent in CIS. A supersystem approach is often believed to be the best approach to obtain the couplings, even if CIS is used. In most cases it is difficult to perform a correlated calculation, so how dynamical correlation can affect the couplings has not been investigated extensively, to the best of our knowledge. The Hartree−Fock method, and consequently CIS, overestimate the charge distribution in molecules and thus overestimate the Coulomb interactions. This is evident in the coupling values, as shown in Table 2, where the coupling is always larger at the CIS level compared to CIS(2). The difference between CIS and CIS(2) is small for the hydrocarbons but quite large for the nucleobases. In particular, for naphthalene and stilbene the CIS and CIS(2) values are almost the same, whereas, at the other extreme, for 2AP they differ by a factor of 2. It seems that dynamical correlation is more important in describing the coupling for nucleobases compared to hydrocarbons. This could be related to the importance of dynamical correlation in describing the mixed character of the excited states of the nucleobases themselves,[45−48] whereas the monomer states in the hydrocarbons are more isolated energetically. The difference between CIS and CIS(2) is often smaller at short range than at long range. The average % dev (Table 3) is 40% at 4 Å, 48% at 8 Å, and 44% at 12 Å. This could be because at short range the other terms besides the Coulomb coupling are present and they can screen the error present in the Coulomb term in CIS.

dx.doi.org/10.1021/jp310603z | J. Phys. Chem. B 2013, 117, 2032−2044

Table 2. Exciton Coupling (eV) Shown for Face-to-Face Dimers at Three Separation Distances, R = 4, 8, and 12 Å for Seven Dimer Systems, T−T, C−C, 2AP−2AP, Hex−Hex, Oct−Oct, Stil−Stil, and Naph−Naph[a]

		tq					pda		
	R/Å	CIS	TDDFT	ZINDO	CIS	CIS(2)	CIS	CIS(2)	TDDFT
T−T	4.0	0.0709	0.0340	0.1083	0.1724	0.1024	0.1803	0.1424	0.0657
	8.0	0.0123	0.0059	0.0190	0.0220	0.0114	0.0225	0.0178	0.0082
	12.0	0.0040	0.0019	0.0061	0.0071	0.0036	0.0067	0.0053	0.0024
C−C	4.0	0.0372	0.0206	0.0599	0.1067	0.0633	0.0926	0.0560	0.0341
	8.0	0.0059	0.0032	0.0094	0.0109	0.0078	0.0116	0.0070	0.0043
	12.0	0.0018	0.0010	0.0029	0.0034	0.0029	0.0034	0.0021	0.0013
2AP−2AP	4.0	0.0573	0.0346	0.0776	0.1255	0.0679	0.1539	0.1017	0.0736
	8.0	0.0107	0.0066	0.0143	0.0165	0.0084	0.0192	0.0127	0.0092
	12.0	0.0035	0.0022	0.0047	0.0053	0.0027	0.0057	0.0038	0.0027
Hex−Hex	4.0	0.1709	0.1522	0.2654	0.4059	0.3561	0.7940	0.6925	0.5663
	8.0	0.0391	0.0350	0.0607	0.0707	0.0545	0.0993	0.0866	0.0708
	12.0	0.0139	0.0124	0.0215	0.0248	0.0192	0.0294	0.0256	0.0210
Oct−Oct	4.0	0.1917	0.1837	0.2902	0.4094	0.3678	1.1900	1.0990	0.9194
	8.0	0.0513	0.0501	0.0777	0.0862	0.0684	0.1488	0.1374	0.1149
	12.0	0.0197	0.0193	0.0297	0.0330	0.0263	0.0441	0.0341	0.0341
Stil−Stil	4.0	0.0852	0.1033	0.1571	0.1831	0.1952	0.5394	0.6247	0.5576
	8.0	0.0233	0.0287	0.0440	0.0389	0.0371	0.0674	0.0781	0.0697
	12.0	0.0089	0.0111	0.0170	0.0149	0.0144	0.0231	0.0200	0.0120
Naph−Naph	4.0	0.0250	0.0259	0.0463	0.1061	0.1205	0.0420	0.0554	0.0360
	8.0	0.0039	0.0043	0.0077	0.0054	0.0050	0.0052	0.0068	0.0045
	12.0	0.0012	0.0013	0.0024	0.0016	0.0015	0.0016	0.0021	0.0013

[a]The basis set used for all methods but ZINDO in this table was cc-pVDZ.

The tq method is expected to work well in describing the coupling for longer distances, because the dominant term is the Coulomb term, whereas it is not expected to work well at short range when the other terms (overlap, exchange, etc.) become important. So we examine the performance of tq's at 8 and 12 Å. A comparison of the tq couplings with the supersystem coupling using the same method, however, does not always show good agreement. The CIS couplings derived from the supersystem are usually larger than the couplings derived from the tq's obtained from CIS. The deviation of the tq couplings from the supersystem CIS values is around 39% on average. Because the couplings of the CIS tq's are always toward smaller values compared to CIS supersystem they seem to correct for the overestimation of the coupling inherent in CIS. So, according to our present results, overall the tq CIS couplings seem to be better than the supersystem CIS couplings because of a systematic cancellation of errors. Actually, the tq CIS couplings agree better with the CIS(2) supersystem values, which are expected to be superior to the CIS ones. The deviation between tq CIS and the reference CIS(2) supersystem couplings is only 13% at R = 8 Å and 15% at R = 12 Å, although the standard deviation is about 25−27% for both distances (Table 3), indicating the sensitivity to the specific type of excitation and molecule. At short distances the deviation increases to 41% on average, consistent with the increased importance of terms beyond the Coulomb term. Even though the overestimation of CIS couplings compared to CIS(2) is expected to be general, it is not clear whether the cancellation of errors observed here will be general, because we do not understand why the fitting gives smaller charge distributions than what CIS predicts.

The tq couplings derived from other methods besides CIS are compared to the CIS(2) supersystem couplings too. Even though one would expect the TDDFT method to be better, and correspondingly the tq charges to perform better than the CIS tq's, this is not the case. For R = 8 Å and R = 12 Å the deviation of tq TDDFT from CIS(2) is 36%, much higher than the deviation seen in CIS tq's (14%, Table 3). The deviation of tq TDDFT from CIS(2), again, depends heavily on the system under study. It is larger for T and C, and smaller for naphthalene. It may be that the much smaller value of the coupling for T and C makes it harder to obtain them accurately. When the Coulomb term is small, it is comparable to the exchange and overlap terms, so the errors of using only the Coulomb approximation are larger.[26] The ZINDO tq couplings also deviate considerably from the CIS(2) coupling at long range for the nucleobases, although they do quite well for short range with these systems, and fairly well for all distances for the hydrocarbons Hex, Oct, and Stil. This could be because of the molecules chosen for the parametrization of the INDO ground state. In general, the couplings generated by tq's depend on the method used to obtain the transition dipole and the charges. Compared to CIS(2) supersystem values, on average, the CIS tq's perform the best, although the behavior depends on the specific chromophore.

PDA couplings generally have larger deviations from the supersystem compared to the couplings generated from tq's, and these deviations get smaller at longer separations. In principle, the difference between PDA and tq's reflects the importance of going beyond the dipole−dipole approximation. However, because we saw earlier that the charges do not reproduce the ab initio TDP, the difference in the coupling also reflects the differences in the transition dipole moment. Therefore, because TDDFT reproduces esTDP much better than CIS does, TDDFT tq's vs TDDFT PDA couplings agree much better with each other compared to CIS tq's vs CIS PDA. The couplings are always lower with tq's, because the tqTDPs are always lower than the esTDPs. To separate the effect of the dipole−dipole approximation, we calculated the PDA coupling using the transition dipole moments obtained from the tq's, and we then compared these couplings to the tq couplings.

dx.doi.org/10.1021/jp310603z | J. Phys. Chem. B 2013, 117, 2032−2044

Table 3. Percent Deviation (% dev) of Coupling from the Supersystem CIS(2) Coupling for All Methods and Values Shown in Table 1[a]

		tq				pda		
	R/Å	CIS	TDDFT	ZINDO	CIS	CIS	CIS(2)	TDDFT
T−T	4.0	−30.79	−66.82	**5.75**	68.28	75.98	39.01	−35.82
	8.0	**7.75**	−48.11	66.55	92.93	97.63	56.11	−27.93
	12.0	**9.13**	−47.47	68.82	96.01	84.34	45.62	−32.77
C−C	4.0	−41.28	−67.43	**−5.47**	68.50	46.15	**−11.63**	−46.10
	8.0	**−25.01**	−59.11	**20.39**	39.17	47.71	**−10.69**	−45.53
	12.0	−36.59	−65.70	**1.42**	**15.68**	**18.36**	−28.43	−56.35
2AP−2AP	4.0	**−15.58**	−48.97	**14.34**	84.80	126.74	49.76	**8.46**
	8.0	27.61	**−21.07**	70.19	96.45	129.77	51.76	**9.91**
	12.0	28.84	**−19.48**	70.96	93.92	108.58	37.77	**−0.23**
Hex−Hex	4.0	−52.00	−57.26	**−25.49**	**13.96**	122.96	94.45	59.01
	8.0	−28.29	−35.81	**11.43**	29.66	82.16	58.87	29.91
	12.0	−27.70	−35.39	**12.10**	29.09	53.07	33.50	**9.17**
Oct−Oct	4.0	−47.87	−50.06	**-21.11**	**11.30**	223.56	198.81	149.98
	8.0	**−24.90**	−26.76	**13.74**	26.11	117.63	100.98	68.14
	12.0	**−25.10**	−26.81	**12.99**	**25.37**	67.45	54.64	29.37
Stil−Stil	4.0	−56.32	−47.08	**−19.48**	**−6.21**	176.39	220.11	185.73
	8.0	−37.31	**−22.55**	**18.70**	**4.86**	81.75	110.50	87.89
	12.0	−38.01	**−23.21**	**18.28**	**3.51**	60.74	38.79	**−16.98**
Naph−Naph	4.0	−79.25	−78.51	−61.58	**−11.95**	−65.15	−54.02	−70.12
	8.0	**−22.00**	**−14.00**	54.00	**8.00**	**4.00**	36.00	**−10.00**
	12.0	**−20.00**	**−13.33**	60.00	**6.67**	**6.67**	40.00	**−13.33**
avg	4.0	−40.64	−56.27	**−8.58**	40.11	128.63	98.42	53.54
std dev	4.0	15.18	9.09	16.14	38.09	64.66	92.64	96.70
avg	8.0	**−13.36**	−35.57	33.50	48.20	92.77	61.26	**20.40**
std dev	8.0	25.26	15.29	27.23	37.74	29.24	43.13	52.38
avg	12.0	**−14.90**	−36.34	**19.58**	43.93	65.42	30.31	**−11.30**
std dev	12.0	27.43	17.52	49.88	40.52	30.38	29.71	30.72

[a]The basis set used for all methods but ZINDO in this table was cc-pVDZ. Bold data are values of % dev where |% dev| is about 25% or less. Also shown are average couplings (avg) for all methods, at all three distances, as well as standard deviations of these averages (std dev).

The difference reduces significantly especially at long distances. The difference depends on the magnitude of the TDP, with the hydrocarbons, which have the largest TDPs, having the largest difference between tq's and PDA, and cytosine, with the smallest TDP, having the smallest difference between tq's and PDA. So the effect of higher multipoles depends on the magnitude of the TDP.

The performance of various quantum mechanical methods in calculating the exciton coupling from the supermolecule has been examined previously.[44] It was found that it is much easier to predict the coupling compared to the excitation energies, and that most ab initio methods predict the coupling reasonably well. In agreement with our results, CIS overestimates the coupling compared to more sophisticated methods that include correlation. The performance of TDDFT has also been examined by other workers,[49] and it was concluded that it is not adequate to calculate the coupling.

The performance of the transition dipole charges has been investigated previously, but using only two systems.[20] It was found that the coupling is reproduced well when compared with that obtained by using the transition densities. The authors also found that it agrees well with supermolecular couplings except at very close distances. Furthermore, they found that the coupling is not very sensitive to which method is used to generate the charges. What we see in our results is that, although these conclusions are true in some chromophores, the degree of agreement and variation depends on the chromophore studied, so it is dangerous to generalize on the basis of studies of one or two molecules.

4.6. Coupling as a Function of Rotation in T. In nature, UV light can induce covalent dimerization of two thymidines which are next to each other in a DNA strand.[50−53] Thus, it is important to be able to theoretically calculate the exciton coupling between two T's in orientations that are similar to those found in DNA, which, on average, are not face-to-face, even when adjacent in the same strand. We defined the term B-DNA rotation in section 3, and it is graphically illustrated in Figure 2. Figure 8 shows the coupling at R = 3.4 Å (the average interbase distance between adjacent base pairs in B-DNA), with B-DNA rotation angles from −40° to +40° (This angle is 35.9° in B-DNA). Couplings using CIS on the dimer, and couplings calculated from T tq's derived from CIS, TDDFT, and ZINDO, are shown. For the supermolecule CIS values the coupling is shown both as half the splitting, and the one obtained from the ER diabatization (denoted ER-CIS). Also shown are PDA using esTDPs from these methods using the equation

$$J = \frac{\boldsymbol{\mu}_1 \cdot \boldsymbol{\mu}_2}{R_{12}^{\,3}} - \frac{3(\boldsymbol{\mu}_1 \cdot \mathbf{R}_{12})(\mathbf{R}_{12} \cdot \boldsymbol{\mu}_2)}{R_{12}^{\,5}} \tag{11}$$

where here $\boldsymbol{\mu}_1$ and $\boldsymbol{\mu}_2$ correspond to the transition dipole vectors of the two T's, R_{12} is the distance between their centers-of-mass, and $\mathbf{R}_{12}$ is the corresponding vector defined by the two centers-of-mass.

When θ = 0°, the T's are face-to-face, and the couplings for all methods are the same as those shown in Figure 4 at R = 3.4 Å. At the small θ values, neither tq nor PDA derived couplings are

dx.doi.org/10.1021/jp310603z | J. Phys. Chem. B 2013, 117, 2032−2044

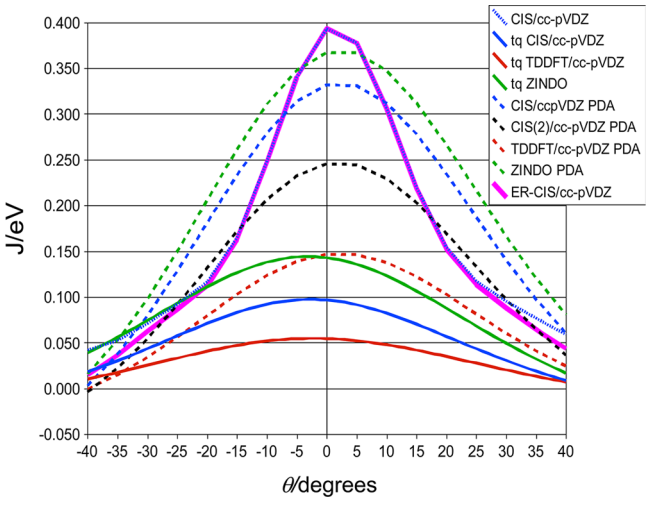

Figure 8. Coupling (eV) shown for a T−T dimer with R = 3.4 Å and B-DNA rotation angle θ, both as defined in section 3, for θ = −40° to +40°. T−T exciton coupling was calculated using CIS/cc-pVDZ, tq's, and PDA from CIS/cc-pVDZ, TDDFT/cc-pVDZ, and ZINDO. CIS/cc-pVDZ is the coupling taken only as the splitting of the relevant states divided by two, and ER-CIS/cc-pVDZ is the coupling obtained with the ER diabatization.

expected to work well, because the non-Coulombic contributions are important. This is obvious in the shape of the curves, which is much steeper for the supermolecular CIS coupling, compared to all other curves. When $|\theta|$ is greater than 20°, the curvature of the tq and PDA couplings better approaches the CIS one.

Couplings from all these methods are also plotted for negative rotation angles, displaying a generally symmetric trend compared to the positive rotation but deviating somewhat due to asymmetries in the distribution of tq's in T, as well as the asymmetric orientation of the esTDPs in the x,y-plane relative to the z-axis.

For T's sharing a strand of B-DNA and separated with one base-pair, R = 6.8 Å and θ = 71.8°. Table 4 shows couplings

Table 4. Exciton Coupling (eV) for a T−T Dimer with Separation of R = 3.4 and 6.8 Å and a B-DNA Rotation Angle θ = 35.9° and 71.8°, As Defined in Section 3

			tq		
R/Å	θ/deg	ER-CIS	CIS	TDDFT	ZINDO
3.4	35.9	0.0600	0.0387	0.0235	0.0659
6.8	71.8	0.0011	0.0006	0.0003	0.0020

using these methods, for the cases of R = 3.4 Å and θ = 35.9°, and R = 6.8 Å and θ = 71.8°, that is, adjacent B-DNA T's and one base-pair separated, respectively. The tq couplings derived from CIS and TDDFT are about a factor of 2 or less than the value of the supermolecular ER-CIS coupling whereas the tq ZINDO coupling is larger. These calculations imply that it is difficult to get accurate couplings for the DNA relevant geometries. Ultimately, only comparison to experiment can verify this, and this information is not currently available.

4.7. Comparisons with Experimental Data of Bichromophores. The work presented here so far tests the ability of tq's to match the supermolecular ab initio values. There is, however, the question of how accurately a supermolecule or tq calculation can reproduce experimental couplings. Experimental determination of the electronic coupling between chromophores is complicated, because there are other factors that can contribute to the observables, such as the vibronic component. Here we discuss two systems shown in Figure 9.

In recent work we have used a single-mode Holstein Hamiltonian to reproduce the absorption, circular dichroism (CD), and photoluminescence in a perylenediimide (PDI) bichromophore.[54] The ability to reproduce the experimental spectra provides a check of the calculated excitonic couplings used in the Holstein Hamiltonian. The system studied was a 1,1′-binaphthalene with a PDI attached by one of the N atoms at the 2 and 2′ positions. This system shall be referred to as PDI_2 and is shown in Figure 9. The details of how the geometry was obtained can be found in the original publication.[54] Transition charges were then calculated for each PDI from a TDDFT S_1 excited state calculation using the B3LYP functional, or a CIS calculation, and the cc-pVDZ basis set. The coupling predicted using tq's derived from the TDDFT transition density is 0.046 eV, whereas the coupling from CIS tq's is similar, 0.048 eV. The predicted spectra using the TDDFT tq coupling agree very well with the experimental ones, verifying that the coupling is quite accurate. Specifically, for the PDI_2 absorption spectrum the ratio of the 0−0 and 1−0 intensities (I_A^{0-0}/I_A^{1-0}) was reproduced, which is very sensitive to the coupling. In addition, the x- and y-polarized spectra, the CD spectrum, and the photoluminescence spectrum were simulated in that study, and all of those were in very good agreement with experiment, highlighting the ability of the tq's to give good coupling. This implies that at least for certain molecules the tq approach can be very accurate and very useful.

The situation is not always as encouraging. To present a fair view of the possible outcomes, we also discuss another system, dithia-anthracenophane (DTA). Yamazaki[55] has reported the total coupling of DTA, including vibronic contributions, by probing the fluorescence anisotropy decay of a THF solution of DTA with a femtosecond up-conversion method. DTA has also been studied theoretically, so it provides a good test molecule to compare the methods used here. Nevertheless, the actual value of the coupling is not yet well established. Experimental values are given as in the order of 15 cm^{-1},[55] whereas theoretical work claims the coupling is closer to 50−100 cm^{-1}, and the deviation from experiment has been attributed to the large phonon−electron coupling.[26]

For this study, DTA was optimized at the MP2/cc-pVDZ level, and the dimethylanthracene dimer, $(DMA)_2$, was generated from the DTA structure by removing the two sulfur atoms, and the connecting bonds with the CH_2 groups were replaced with reasonable C−H bonds, making two methyl groups on each separate anthracene. Their structures are shown in Figure 9. Data for DTA and the general $(DMA)_2$ systems are given in Table 5. Here the anthracenes are roughly parallel to each other, and the two anthracene long axes are oriented approximately 90° to each other. In the crystal structure of DTA they are separated by 3.41 Å, whereas at the MP2/cc-pVDZ level of optimization of DTA they are 3.19 Å apart. Thus, for comparison, the interanthracene couplings were studied at both of these distances, using all methods described here for calculation of excitonic coupling. A CIS calculation of the ground state MP2 geometry of DTA showed that removing the sulfur links to create DMAs having the same anthracene geometries, orientations and separation had little effect on the coupling as compared to the full DTA system used to generate

dx.doi.org/10.1021/jp310603z | J. Phys. Chem. B 2013, 117, 2032−2044

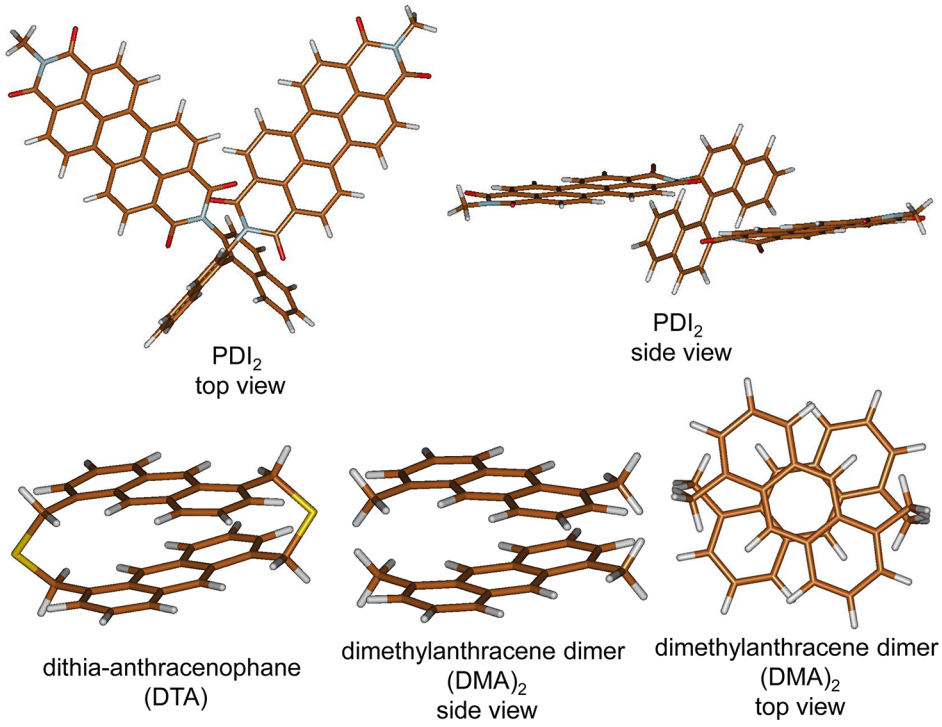

Figure 9. Structures of molecules presented in section 4.7, along with their names and abbreviations used.

Table 5. DTA and $(DMA)_2$ Coupling Data[a]

	R = 3.19 Å		R = 3.41 Å	
	V/eV	V/cm^{-1}	V/eV	V/cm^{-1}
DTA expt (THF)[55]			0.00177	14.3 (50−100)
$(DMA)_2$ CIS/cc-pVDZ	0.02905	234.3	0.01730	139.5
$(DMA)_2$ tq's CIS/cc-pVDZ	0.00410	33.1	0.00353	28.5
$(DMA)_2$ tq's TDDFT/cc-pVDZ	0.00250	20.1	0.00219	17.6
$(DMA)_2$ tq's ZINDO	0.00884	71.3	0.00781	63.0

[a]Shown are J couplings of $(DMA)_2$ created from the MP2/cc-pVDZ DTA minimum, at two inter-anthracene distances, 3.19 and 3.41 Å, from tq's and supermolecule calculations. The experimental coupling of DTA[55] is given for comparisons.

the DMAs, indicating the small effect of through-bond coupling. The experimentally determined total coupling is given in Table 5 as 14.3 cm^{-1}. However, theoretical work which modeled the coherent resonance energy transfer[26] suggests that this is the effective coupling and the actual electronic coupling is much larger, 50−100 cm^{-1}.

Our predicted theoretical results are shown in Table 5. If one believes the value to be 50−100 cm^{-1}, it is seen that the supermolecular approach overestimates the coupling whereas the tq approach underestimates it. If one, however, assumes the original experimental value to be correct, then the tq method does much better than the supermolecular. In fact, the supermolecular approach gives values that are an order of magnitude larger. The deviation between tq's and supermolecule couplings is much larger here than any of the other systems studied in this work, indicating that it is harder to describe the coupling in this system.

Another important point to be seen in Table 5 is the influence of the geometry on predicting an accurate coupling. If the theoretical geometry is used to estimate the coupling, the value almost doubles for certain methods. This is important considering that often the experimental crystal structure is not available and one has to rely on the theoretical geometry. The sensitivity of the coupling on the geometry on DTA has been discussed by others as well.[26]

A recent study highlights the effect of vibronic coupling in the discrepancies between theory and experiment.[56] High accuracy spectroscopic data combined with theory on gas phase dimers were used to benchmark the splittings. It was found that the ab initio couplings were 10−40 times larger than the experimentally measured couplings. As the authors point out, the problem is that the excitonic splittings arise between the vibronic (and not the electronic) transitions, and the monomer electronic-vibrational coupling upon electronic excitation must be accounted for.

5. CONCLUSIONS

We have presented the results of calculated excitonic couplings for a variety of chromophores as homodimers, using various single-reference ab initio excited state methods, as well as a semiempirical method. Transition charges using these methods were derived with a Mulliken population analysis of the transition densities of each of these methods, and the Coulombic interchromophore couplings were calculated and compared to supermolecule derived couplings, as well as the point-dipole approximation.

Our calculations show that it is much easier to calculate quantum mechanically the exciton coupling compared to the excitation energies. The variations in the excitation energies when different quantum mechanical methods are used can be in the order of one or more eV, whereas the variations in the couplings are usually less than one-tenth of an electronvolt.

In general, couplings from transition charges compare quite favorably to the supermolecule values at interchromophore separations R > 4.5 Å, but at close distances ab initio methods

dx.doi.org/10.1021/jp310603z | J. Phys. Chem. B 2013, 117, 2032−2044

treating the full dimer display much larger couplings than the transition charge methods because the Coulomb interaction is no longer the main one. None of the three methods studied here, CIS, TDDFT, or ZINDO, is clearly outperforming the other two in obtaining tq's and couplings. Their respective accuracy depends on the system studied. The effect of the basis set used in the monomer calculation on the derived tq's and couplings is minimal, allowing the use of smaller basis sets without loss of accuracy.

We also observed that in certain cases the tq coupling may be better than a supermolecular coupling, which is advantageous because one can get the tq couplings at a fraction of the effort required for a supermolecule calculation. Our results indicate that this may occur because of cancellation of errors. In particular, CIS derived tq's are likely to predict better couplings than a supermolecule CIS calculations. This is because tq's derived from a given method underestimate the TDP produced quantum mechanically by the same method, and thus they underestimate the Coulomb coupling compared to the supersystem. On the other hand, CIS overestimates the TDP and Coulomb interactions, so the tq's derived from CIS bring the coupling toward the right direction. Though the latter is expected to be general, there is no general proof that the former behavior of tq charges will be general. If the current trends, however, persist in other systems, it suggests that fortuitous cancellations of errors may allow very inexpensive CIS or TDDFT monomer-based transition charges obtained from Mulliken population analysis to be quite accurate in predicting excitonic coupling, which undoubtedly will be most useful to a wide variety of researchers studying the spectral properties of aggregates of very large chromophores, both in the nanotechnology field as well as the biological sciences.

Comparisons with experiment are challenging, because it is difficult to directly observe the coupling experimentally. Indirect comparisons indicate that there are cases where the tq couplings are very accurate, and this is a very efficient way to obtain couplings. On the other hand, there are cases where it is more challenging to reproduce the experimental coupling even when more accurate ab initio methods are used.

AUTHOR INFORMATION

Corresponding Authors

*E-mail: kak46@psu.edu.

‡E-mail: smatsika@temple.edu.

Present Address

†Department of Chemistry, Pennsylvania State University, Brandywine Campus, Media, PA 19063.

Notes

The authors declare no competing financial interest.

ACKNOWLEDGMENTS

This work was supported by the National Science Foundation under grants CHE-1213614 and DMR-1203811. We also thank Dr. Stan Smith for guidance in utilizing Gaussian03 to obtain usable matrix information used in this study.

ACRONYMS

2AP	2-amino-9-methylpurine
3-21G	minimum Gaussian-based basis set
AO	atomic orbital
aug-cc-pVDZ	Dunning's correlation-consistent polarizable double-ζ basis set with diffuse functions
C	1-methylcytosine
cc-pVDZ	Dunning's correlation-consistent polarizable double-ζ basis set
cc-pVTZ	Dunning's correlation-consistent polarizable triple-ζ basis set
CD	circular dichroism
CI	configuration interaction
CIS	configuration interaction singles
CIS(2)	CIS method with second-order perturbation theory to include double excitations
CT	charge transfer
DMA	dimethylanthracene
$(DMA)_2$	dimer of DMA
DTA	dithia-anthracenophane
ER	Edmiston−Ruedenberg
ER-CIS	application of ER diabatization on CIS
esTDP	transition dipole from the electronic structure calculation
f	oscillator strength
Hex	*S-trans*-1,3,5-hexatriene
INDO	intermediate neglect of differential overlap (Semiempirical method)
J	coupling
MO	molecular orbital
MP2	Moller−Plessett second-order perturbation theory
MPA	Mulliken population analysis
Naph	naphthalene
Oct	*S-trans*-1,3,5,7-octatetraene
PDA	point dipole approximation
PDA CIS	dimer exciton coupling based on monomeric CIS transition dipoles
PDA CIS(2)	dimer exciton coupling based on monomeric CIS(2) transition dipoles
PDA TDDFT	dimer exciton coupling based on monomeric TDDFT transition dipoles
PDI	perylenediiimide
PDI_2	bichromophore with two PDIs connected by a binaphthene
Stil	*trans*-stilbene
STO-3G	minimum ortho-normal Slater-type orbital basis set used by ZINDO
T	1-methylthymine
TDDFT	time-dependent density functional theory
TDP	transition dipole
tq	trasition charge centered on an atom
ltql	magnitude of transition charge
tq CIS	dimer exciton coupling from monomeric CIS-derived tq's
tq TDDFT	dimer exciton coupling from monomeric TDDFT-derived tq's
tq ZINDO	dimer exciton coupling from monomeric ZINDO-derived tq's
tqTDP	transition dipole based on transition charges
ZINDO	CIS based on the INDO ground state using Zerner's method

REFERENCES

(1) Schwartz, E.; Palermo, V.; Finlayson, C. E.; Huang, Y.-S.; Otten, M. B. J.; Liscio, A.; Trapani, S.; González-Valls, I.; Brocorens, P.; Cornelissen, J. J. L. M.; et al. *Chem.—Eur. J.* **2009**, *15*, 2536−2547.

(2) Spano, F. C.; Meskers, S. C. J.; Hennebicq, E.; Beljonne, D. *J. Am. Chem. Soc.* **2007**, *129*, 7044−7054.

(3) Cheng, Y. C.; Silbey, R. J. *Phys. Rev. Lett.* **2006**, *96*, 028103 1−4.
(4) Cheng, Y.-C.; Fleming, G. R. *Annu. Rev. Phys. Chem.* **2009**, *60*, 241−262.
(5) Crespo-Hernandez, C. E.; Cohen, B.; Kohler, B. *Nature* **2005**, *436*, 1141−1144.
(6) Frenkel, J. *Phys. Rev.* **1931**, *37*, 1276−1294.
(7) Scholes, G. D.; Ghiggino, K. P. *J. Phys. Chem.* **1994**, *98*, 4580−4590.
(8) Chang, J. C. *J. Chem. Phys.* **1977**, *67*, 3901−3909.
(9) Krueger, B. P.; Scholes, G. D.; Fleming, G. R. *J. Phys. Chem. B* **1998**, *102*, 5378−5386.
(10) Hsu, C.-P.; Graham, R. F.; Head-Gordon, M.; Head-Gordon, T. *J. Chem. Phys.* **2001**, *114*, 3065−3072.
(11) Hsu, C.-P.; Walla, P. J.; Head-Gordon, M.; Fleming, G. R. *J. Phys. Chem. B* **2001**, *105*, 11016−11025.
(12) Vura-Weis, J.; Newton, M. D.; Wasielewski, M. R.; Subotnik, J. E. *J. Phys. Chem. C* **2010**, *114*, 20449−20460.
(13) Wong, C. Y.; Curutchet, C.; Tretiak, S.; Scholes, G. D. *J. Chem. Phys.* **2009**, *130* (081104), 1−4.
(14) Beljonne, D.; Cornil, J.; Silbey, R.; Millie, P.; Bredas, J. L. *J. Chem. Phys.* **2000**, *112*, 4749−4758.
(15) Beljonne, D.; Pourtois, G.; Silva, C.; Hennebicq, E.; Herz, L. M.; Friend, R. H.; Scholes, G. D.; Setayesh, S.; Mullen, K.; Bredas, J. L. *Proc. Natl. Acad. Sci.* **2002**, *99*, 10982−10987.
(16) Beenken, W. J. D.; Pullerits, T. *J. Chem. Phys.* **2004**, *120*, 2490−2495.
(17) Patwardhan, S.; Sengupta, S.; Würthner, F.; Siebbeles, L. D. A.; Grozema, F. *J. Phys. Chem. C* **2010**, *114*, 20834−20842.
(18) Bouvier, B.; Gustavsson, T.; Markovitsi, D.; Millié, P. *Chem. Phys.* **2002**, *275*, 75−92.
(19) Madjet, M. E.; Abdurahman, A.; Renger, T. *J. Phys. Chem. B* **2006**, *110*, 17268−17281.
(20) Howard, I. A.; Zutterman, F.; Deroover, G.; Lamoen, D.; Van Alsenoy, C. *J. Phys. Chem. B* **2004**, *108*, 19155−19162.
(21) Li, H.; Malinin, S. V.; Tretiak, S.; Chernyak, V. Y. *J. Chem. Phys.* **2010**, *132* (124103), 1−9.
(22) Iozzi, M. F.; Mennucci, B.; Tomasi, J.; Cammi, R. *J. Chem. Phys.* **2004**, *120*, 7029−7040.
(23) Hsu, C.-P.; You, Z.-Q.; Chen, H.-C. *J. Phys. Chem. C* **2008**, *112*, 1204−1212.
(24) Muñoz Losa, A.; Curutchet, C.; Krueger, B. P.; Hartsell, L. R.; Mennucci, B. *Biophys. J.* **2009**, *96*, 4779−4788.
(25) Speelman, A. L.; Munoz-Losa, A.; Hinkle, K. L.; VanBeek, D. B.; Mennucci, B.; Krueger, B. P. *J. Phys. Chem. A* **2011**, *115*, 3997−4008.
(26) Yang, L.; Caprasecca, S.; Mennucci, B.; Jang, S. *J. Am. Chem. Soc.* **2010**, *132*, 16911−16921.
(27) Longuet-Higgins, H. C. *Proc. R. Soc. London A* **1956**, *235*, 537−543.
(28) Frisch, M. J.; Trucks, G. W.; Schlegel, H. B.; Scuseria, G. E.; Robb, M. A.; Cheeseman, J. R.; Montgomery, J.; Vreven, T.; Kudin, K. N.; Burant, J. C.; et al. *Gaussian 03*, revision a.1; Gaussian: Wallingford, CT, 2003.
(29) Frisch, M. J.; Trucks, G. W.; Schlegel, H. B.; Scuseria, G. E.; Robb, M. A.; Cheeseman, J. R.; Scalmani, G.; Barone, V.; Mennucci, B.; Petersson, G. A.; et al. *Gaussian 09*, Revision A.1; Gaussian: Wallingford, CT, 2009.
(30) Dunning, T. H. *J. Chem. Phys.* **1989**, *90*, 1007−1023.
(31) Laikov, D.; Matsika, S. *Chem. Phys. Lett.* **2007**, *448*, 132−137.
(32) Kozak, C. R.; Kistler, K. A.; Lu, Z.; Matsika, S. *J. Phys. Chem. B* **2010**, *114*, 1674−1683.
(33) Hsu, C.-P. *Acc. Chem. Res.* **2008**, *42*, 509−518.
(34) Subotnik, J. E.; Yeganeh, S.; Cave, R. J.; Ratner, M. A. *J. Chem. Phys.* **2008**, *129* (244101), 1−10.
(35) Subotnik, J. E.; Cave, R. J.; Steele, R. P.; Shenvi, N. *J. Chem. Phys.* **2009**, *130* (234102), 1−14.
(36) Shao, Y.; Fusti-Molnar, L.; Jung, Y.; Kussmann, J.; Ochsenfeld, C.; Brown, S. T.; Gilbert, A. T. B.; Slipchenko, L. V.; Levchenko, S. V.; O'Neill, D. P.; et al. *Phys. Chem. Chem. Phys.* **2006**, *8*, 3172.
(37) Schmidt, M. W.; Baldridge, K. K.; Boatz, J. A.; Elbert, S. T.; Gordon, M. S.; Jensen, J. J.; Koseki, S.; Matsunaga, N.; Nguyen, K. A.; Su, S.; et al. *J. Comput. Chem.* **1993**, *14*, 1347−1363.
(38) Schaftenaar, G.; Noordik, J. H. *J. Comput.-Aided Mol. Des.* **2000**, *14*, 123−134.
(39) Bode, B. M.; Gordon, M. *J. Mol. Graphics Modell.* **1998**, *16*, 133−138.
(40) Priroda documentation. Laikov, D. N. 2008.
(41) Gavin, R. M.; Salomon, R.; Stuart, A. R. *J. Chem. Phys.* **1973**, *58*, 3160−3165.
(42) Gavin, R. M.; Charles, W.; Jeffrey, K. M.; Stuart, A. R. *J. Chem. Phys.* **1978**, *68*, 522−529.
(43) Cramer, C. J. *Essentials of Computational Chemistry, Theories and Models*; John Wiley & Sons, Ltd.: West Sussex, England, 2002.
(44) Muñoz Losa, A.; Curutchet, C.; Galván, I. F.; Mennucci, B. *J. Chem. Phys.* **2008**, *129* (034104), 1−16.
(45) Matsika, S. *J. Phys. Chem. A* **2004**, *108*, 7584−7590.
(46) Kistler, K. A.; Matsika, S. *Photochem. Photobiol.* **2007**, *83*, 611−624.
(47) Kistler, K. A.; Matsika, S. *J. Phys. Chem A* **2007**, *111*, 2650−2661.
(48) Epifanovsky, E.; Kowalski, K.; Fan, P.-D.; Valiev, M.; Matsika, S.; Krylov, A. I. *J. Phys. Chem. A* **2008**, *112*, 9983−9992.
(49) Liu, W.; Settels, V.; Harbach, P. H. P.; Dreuw, A.; Fink, R. F.; Engels, B. *J. Comput. Chem.* **2011**, *32*, 1971−1981.
(50) Cadet, J.; Sage, E.; Douki, T. *Mutat. Res.* **2005**, *571*, 3−17.
(51) Pfeifer, G. P.; You, Y.-H.; Besaratinia, A. *Mutat. Res., Fundam. Mol. Mech. Mutagen.* **2005**, *571*, 19−31.
(52) Boggio-Pasqua, M.; Groenhof, G.; Schäfer, L. V.; Grubmüller, H.; Robb, M. A. *J. Am. Chem. Soc.* **2007**, *129*, 10996−10997.
(53) Hariharan, M.; Lewis, F. D. *J. Am. Chem. Soc.* **2008**, *130*, 11870−11871.
(54) Kistler, K. A.; Pochas, C. M.; Yamagata, H.; Matsika, S.; Spano, F. C. *J. Phys. Chem. B* **2012**, *116*, 77−86.
(55) Yamazaki, I.; Akimoto, S.; Yamazaki, T.; Sato, S.; Sakata, Y. *J. Phys. Chem. A* **2002**, *106*, 2122−2128.
(56) Ottiger, P.; Leutwyler, S.; Köppel, H. *J. Chem. Phys.* **2012**, *136*, 174308 1−13.
(57) Clark, L. B.; Peschel, G. G.; I. Tinoco, J. *J. Phys. Chem.* **1965**, *69*, 3615−3618.
(58) Abouaf, R.; Pommier, J.; Dunet, H.; Quan, P.; Nam, P.-C.; Nguyen, M. T. *J. Chem. Phys.* **2004**, *121*, 11668−11674.
(59) Holmén, A.; Nordén, B.; Albinsson, B. *J. Am. Chem. Soc.* **1997**, *119*, 3114−3121.
(60) Flicker, Wayne M., M. O. A.; Kuppermann, A. *Chem. Phys. Lett.* **1977**, *45*, 492−497.
(61) Bouwman, W. G.; Jones, A. C.; Phillips, D.; Thibodeau, P.; Friel, C.; Christensen, R. L. *J. Phys. Chem.* **1990**, *94*, 7429−7434.
(62) Gudipati, M. S.; Maus, M.; Daverkausen, J.; Hohlneicher, G. *Chem. Phys.* **1995**, *192*, 37−47.
(63) Klevens, H.; Platt, J. *J. Chem. Phys.* **1949**, *17*, 470−484.
(64) George, G. A. *J. Mol. Spectrosc.* **1968**, *26*, 67−71.